The oxygen-assisted transformation of propane to CO_x/H_2 through combined oxidation and WGS reactions catalyzed by vanadium oxide-based catalysts

N. Ballarini [a,1], A. Battisti [a,1], F. Cavani [a,1,*], A. Cericola [a,1], C. Lucarelli [a,1], S. Racioppi [a,1], P. Arpentinier [b]

[a] Dipartimento di Chimica Industriale e dei Materiali, Viale Risorgimento 4, INSTM, Research Unit of Bologna, 40136 Bologna, Italy
[b] Air Liquide, Centre de Recherche Claude Delorme, les Loges en Josas, 78354 Jouy-en-Josas Cedex, France

Abstract

This paper reports about the gas-phase oxidation of propane catalyzed by bulk vanadium oxide and by alumina- and silica-supported vanadium oxide. The reaction was studied with the aim of finding conditions at which the formation of H_2 and CO_2 is preferred over that of CO, H_2O and of products of alkane partial oxidation. It was found that with bulk V_2O_5 considerable amounts of H_2 are produced above 400 °C, the temperature at which the limiting reactant, oxygen, is totally consumed. The formation of H_2 derived from the combination of: (i) oxidation reactions, with generation of CO, CO_2, oxygenates (mainly acetic acid), propylene and H_2O, all occurring in the fraction of catalytic bed that operated in the presence of gas-phase oxygen, and (ii) WGS reaction, propane dehydrogenation and coke formation, that instead occurred in the fraction of bed operating under anaerobic conditions. This combination of different reactions in a single catalytic bed was possible because of the reduction of V_2O_5 to V_2O_3 at high temperature, in the absence of gas-phase oxygen. In fact, vanadium sesquioxide was found to be an effective catalyst for the WGS, while V_2O_5 was inactive in this reaction. The same combination of reactions was not possible when vanadium oxide was supported over high-surface area silica or alumina; this was attributed to the fact that in these catalysts vanadium was not reduced below the oxidation state V^{4+}, even under reaction conditions leading to total oxygen conversion. In consequence, these catalysts produced less H_2 than bulk vanadium oxide.
© 2006 Elsevier B.V. All rights reserved.

Keywords: Vanadium oxide; Supported vanadium oxide; Propane oxidation; Hydrogen production; WGS reaction

1. Introduction

The use of oxygen in processes for H_2 production from hydrocarbons transformation is aimed either at directly furnishing the reaction heat from the inside of the reactor, like in autothermal reforming, or at facilitating a specific reaction pathway other than combustion, like in methane (alkanes) partial oxidation [1–12]. For instance, the addition of oxygen to reformers or WGS reactors is a tool to increment the hydrogen concentration and facilitate CO transformation to CO_2. The catalysts employed for these reactions are often based on noble metals, capable of activating less reactive hydro-carbons and perform the desired transformations. Other approaches include the use of metal oxides (e.g., Fe_2O_3) for the combustion of methane to CO_2 in the absence of gas-phase oxygen, followed by the re-oxidation of Fe with H_2O to produce H_2 (the One-Step-Hydrogen process) [13,14], or the co-production of coke and H_2 from the contact of methane with Ni-based systems or supported noble metal catalysts, followed by coke combustion with O_2 [15].

Very few indications are given in literature concerning the use of vanadium oxide-based catalysts for the transformation of light hydrocarbons into CO_2 and H_2. Vanadium oxide is a key component in the preparation of catalysts for oxidation reactions [16–20]. It is used either as a supported active phase, to increase its surface area, or in combination with other ions to form mixed oxides, in order to obtain a system with modified and enhanced oxo-reductive properties. In the case of alkanes oxidation, catalysts based on supported vanadium

oxide are often studied for the synthesis of light olefins by means of oxidehydrogenation (ODH) [21–26]. It is believed that the reaction mechanism includes the dehydrogenation of alkanes with co-production of water, while little attention is given to the formation of H_2. Indeed, in most cases ODH is carried out using O_2 as the limiting reactant, since hydrocarbon-rich conditions may lead to a better selectivity to the olefin. This implies that total conversion of oxygen is reached, especially when temperatures higher than 500 °C are used. Under these conditions, a relevant contribution of catalytic dehydrogenation to H_2 formation cannot be excluded. Recent papers confirm that considerable amounts of H_2 are produced with vanadium oxide-based catalysts, under conditions that are typically employed for alkanes ODH [27–32].

In the present work, we report about the investigation on catalytic properties of bulk and supported vanadium oxide catalysts in the oxidation of propane, with the aim of finding whether the active phase properties and the reaction conditions may affect the mechanism in propane oxidation, and the amount of H_2 produced.

2. Experimental

Commercial vanadium pentoxide was supplied by Aldrich (>99.6%). Supported catalysts were prepared with the incipient-wetness technique using γ-alumina powder (AKZO A4) or silica (Sud-Chemie), and an aqueous solution of NH_4VO_3. Samples were calcined in air at 550 °C. Table 1 reports the list of samples prepared, and the corresponding values of surface area. The two supports were chosen so to achieve comparable values of surface areas for the two series of samples.

Catalytic tests were carried out in a quartz, fixed-bed reactor loading 1.8 cm^3 of catalyst in powder form (30–40 mesh particles), at atmospheric pressure. Tests of propane oxidation were carried out by feeding a mixture containing 20% propane, 20% oxygen and remainder He. Residence time was equal to 2 s, and was calculated with reference to the entire amount of catalyst (active phase + support, when present). Catalytic tests of WGS reaction were carried out by feeding a mixture containing 9% H_2O, 9% CO and remainder N_2.

Reaction products of propane oxidation were carbon monoxide, carbon dioxide, light hydrocarbons (ethane, ethylene, methane), aromatics, oxygenates (acetaldehyde, propionalde-

hyde, acetone, acrolein, acetic acid, acrylic acid and propionic acid), molecular hydrogen, propylene and water (not analysed). The effluents were analysed by a gas chromatograph equipped with three packed columns: (i) Carbosieve G (TCD) for the analysis of hydrogen, oxygen, carbon monoxide and carbon dioxide; (ii) fused silica Al_2O_3/KCl (FID) for propylene, propane and other hydrocarbons; (iii) Econopak/EC-Wax (FID) for the oxygenated compounds.

Catalysts were characterized by laser Raman spectrometry (Renishaw 1000 instrument, Ar laser at 514 nm, power 25 mW). The amount of residual C content in samples was determined by combustion in pure oxygen at 1300 °C, with detection of the CO_2 formed by infrared analysis (instrument ELTRA 900CS). Thermal-programmed-reduction (TPR) analysis of samples was carried out using a Thermoquest TPDRO1100 instrument. Samples were loaded in a quartz reactor and pre-treated in nitrogen at 150 °C for 30 min to eliminate weakly adsorbed species. After cooling at room temperature, N_2 was replaced by the analyzing gas (5% H_2 in argon) and the temperature was linearly increased up to 650 °C (thermal ramp: 10 °C/min); the samples were finally maintained at 650 °C for 1 h. TPO and TPR-O (re-oxidation after TPR) tests were carried out using a gas mixture of 5% O_2 in He, using the same temperature program as for the reduction.

3. Results and discussion

3.1. The effect of temperature on catalytic performance in propane oxidation of vanadium oxide-based catalysts

Table 1 summarizes the main characteristics of samples; two series of catalysts were prepared by supporting increasing amounts of ammonium vanadate on silica or on alumina. Furthermore, a sample of unsupported bulk V_2O_5 (bulkVO) was used as the reference.

Fig. 1 compares the conversion of propane and of oxygen as functions of temperature, for samples bulkVO, SiV15 and AlV15. Under the conditions employed, oxygen was the

Table 1
Catalysts prepared

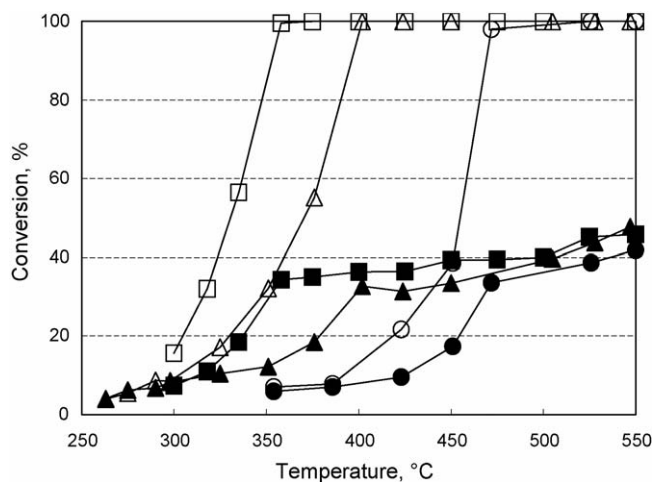| Sample	V_2O_5 (wt.%)	Support	Surface area (m^2/g)
SiV2	2	SiO_2	280
SiV7	7	SiO_2	274
SiV10	10	SiO_2	259
SiV15	15	SiO_2	254
AlV2	2	γ-Al_2O_3	234
AlV7	7	γ-Al_2O_3	227
AlV10	10	γ-Al_2O_3	215
AlV15	15	γ-Al_2O_3	191
bulkVO	100	None	8

Fig. 1. Conversion of propane (full symbols) and conversion of oxygen (open symbols) as functions of the reaction temperature. Catalysts: SiV15 (●), AlV15 (■) and bulkVO (▲).

limiting reactant. Despite the same amount of vanadium oxide, and the comparable value of surface area, the two supported catalysts had different activity. Sample AlV15 was the most active, and reached total conversion of oxygen already at 350 °C, that is 100° less than for the silica-supported system. Very surprising was the high activity of bulkVO, despite its very low surface area; total conversion of oxygen was reached at 400 °C. The only possible explanation for this phenomenon is that within the redox cycle the removal of the O^{2-} species at the surface is followed by a quick migration of the latter from the inner bulk, so providing a high turnover frequency for the limited number of surface V sites.

The differences in activity for the two supported catalysts can be attributed to the different nature of the active species that form when vanadium oxide is impregnated on silica and on alumina. While polyvanadates develop on alumina, in the case of silica bulk vanadium oxide begins to form well below the theoretical amount necessary to reach a complete support coverage [19,33–36]. With all supports, isolated tetrahedral VO_x species form when a low vanadium oxide loading is used. Moreover, also the redox properties of V species can be greatly affected by the nature of the interaction that develops between the active phase and the support [36].

Notwithstanding the total conversion of oxygen, with all catalysts a further increase of propane conversion was observed above 450 °C; this was due to the contribution of dehydrogenation to the conversion of the alkane.

Details concerning the effect of temperature on the selectivity to the different products are given in Figs. 2–4 for bulkVO, SiV15 and AlV15, respectively. In the case of bulkVO, two temperature zones can be identified, (i) below 400 °C and (ii) above 400 °C, each one with a different distribution of the products. In the range between 250 and 400 °C, the main product of partial oxidation was propylene, but its selectivity decreased from 20 to 7% when the temperature was raised from 275 to 400 °C; the selectivity to CO and CO_2 correspondingly increased. Little amounts of oxygenated compounds formed: mainly acetaldehyde and

Fig. 3. Selectivity to the products and H_2 concentration in the exit stream as functions of the reaction temperature. Catalyst: SiV15. Symbols as in Fig. 2.

acetone, with minor formation of acetic acid, acrylic acid, propionaldehyde, propionic acid and acrolein. The analysis of the sample downloaded after reaction in this temperature range indicated that no coke had deposited over the catalyst surface.

Above 400 °C, oxygen was totally consumed. In between 400 and 450 °C, propane conversion was constant; then, it progressively increased up to 48% at 550 °C. Propylene selectivity slightly increased, due to the contribution of dehydrogenation, but never reached values higher than 12%. In this interval, hydrogen was produced in non-negligible amount; at 550 °C, it reached a concentration of 9.1% in the outlet stream. Selectivity to CO reached a maximum value at 400 °C and then decreased, while the formation of CO_2 increased in the 400–500 °C range, notwithstanding total oxygen conversion. In this temperature range, also small amounts of aromatics (mainly toluene), and aliphatic hydrocarbons (methane, ethane, ethylene, and heavier than propane as well) formed, with an overall selectivity lower than 8%. The amount of coke accumulated on the catalyst in a few hours of reaction was equal to 0.65 wt.% C, as inferred from the analysis of the sample downloaded after reaction at 550 °C.
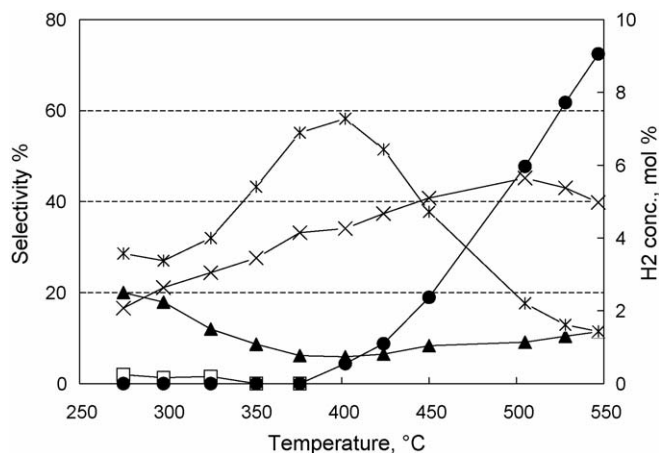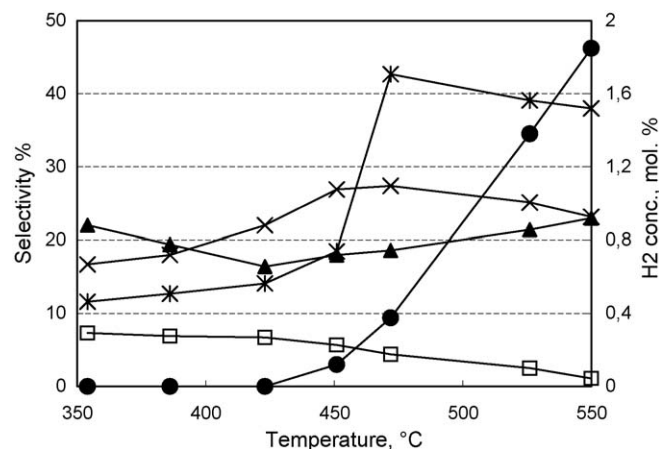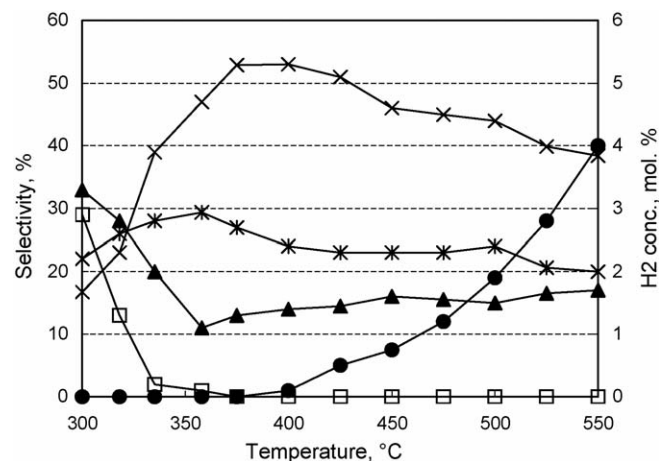

Fig. 2. Selectivity to the products and H_2 concentration in the exit stream as functions of the reaction temperature. Catalyst: bulkVO. Symbols: oxygenates (□), propylene (▲), CO (✳), CO_2 (×) and H_2 (●).
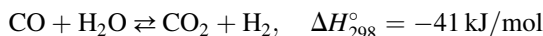

Fig. 4. Selectivity to the products and H_2 concentration in the exit stream as functions of the reaction temperature. Catalyst: AlV15. Symbols as in Fig. 2.

It is worth noting that the results plotted in Fig. 2 were obtained after 3–4 h reaction, for each temperature level. The formation of coke under conditions of total oxygen conversion implied a C balance (as calculated on the basis of the composition of the outlet gaseous stream) that was lower than 100%. Moreover, a progressive variation of catalytic performance during the elapsing time-on-stream should be expected, due to the modification of catalyst surface as a consequence of C deposition. However, tests aimed at monitoring the performance during the first hours of reaction evidenced that the unsteady catalytic behaviour at high temperature lasted less than 1 h. In this period, during which coke began to accumulate on catalyst surface in the fraction of bed that operated in the absence of oxygen, the propane and oxygen conversions first decreased and then increased again, and finally became similar to the starting values. Furthermore, the distribution of products remained substantially stable during this initial period.

Both propane dehydrogenation and coke formation are endothermic reactions, favoured at temperatures higher than 400 °C. Nevertheless, the amount of H_2 obtained was higher than that expected on the basis of these two reactions only. One reaction that can justify the additional amount of hydrogen formed and, at the same time, the opposite trends of CO and CO_2, is WGS:

$$CO + H_2O \rightleftarrows CO_2 + H_2, \quad \Delta H^{\circ}_{298} = -41 \text{ kJ/mol}$$

The distribution of products obtained with silica-supported and alumina-supported samples (Figs. 3 and 4) had analogies with that one obtained with bulk vanadium oxide, but also remarkable differences. In the case of SiV15, for temperatures lower than that of total oxygen conversion, the catalytic performance was similar to that of bulkVO. The selectivity to carbon oxides increased while that to propylene slightly decreased. In this range the C balance was low, comprised between 50 and 60%; this was due to the formation of a heavier by-product, that was found by GC analysis but was not identified. However, the C balance was close to 100% (and, correspondingly, there was no formation of the heavy by-product) at 450–470 °C, when oxygen conversion was total.

We made the hypothesis that the heavy by-product might form by consecutive transformation of propylene. However, tests made by feeding 3% propylene and 20% O_2 at 354 °C gave the following results: propylene conversion 46%, selectivity to acetaldehyde 21%, to acetone 20%, to CO 13% and to CO_2 38%, with negligible formation of the heavy by-product.

In the case of AlV15, the selectivity to propylene and to oxygenated compounds (mainly acetic acid and acetaldehyde) was higher than that obtained with bulkVO and SiV15. Both however declined when the temperature was increased, with a corresponding increase in CO_x formation. The major difference between SiV15 and AlV15 concerned the C balance; in the latter case, there was no formation of the heavy by-product at low temperature, and in fact the C balance was close to 90–100%.

However, the greater difference between supported samples and bulkVO was found at temperatures higher than those at which total conversion of oxygen was reached. It is shown that

with supported catalysts the selectivity to CO and that to CO_2 did not show the opposite trends observed in the case of bulkVO. For both SiV15 and AlV15 the selectivity to carbon oxides declined when the temperature was raised, while the selectivity to propylene increased, due to the contribution of propane dehydrogenation to the formation of the olefin. Therefore, in this temperature range the two supported samples had a similar distribution of products, different from that one of bulkVO. The concentration of hydrogen in the outlet stream was considerably lower than that obtained with bulkVO.

It is worth noting that the C balance calculated in the 500–550 °C temperature range was around 70–75% for bulkVO, 75–80% for AlV15 and 90% for SiV15. This indicates that the formation of coke was the higher with the bulk catalyst, whereas it was the lower with the silica-supported system. Since the formation of coke also contributed to H_2 production, this can explain the different amount of H_2 produced for SiV15 and AlV15. On the other hand, the slightly higher amount of coke that formed with bulkVO is not sufficient to justify the considerably higher concentration of H_2 obtained with this catalyst. It is clear that the main reason for this difference was the presence of the WGS reaction, that greatly contributed to H_2 formation in the case of bulkVO, while was substantially absent with both supported samples.

3.2. Further insights into the reactivity of bulk vanadium oxide in propane oxidation

BulkVO was characterized by X-ray diffraction after catalytic tests made at different temperatures: (i) at 370 °C, that is, at yet not complete oxygen conversion, (ii) at 400 °C, when total oxygen conversion was reached and (iii) at 550 °C, the highest reaction temperature. Corresponding diffraction patterns are shown in Fig. 5. The patterns of fresh sample and of the catalyst after reaction at 370 °C were identical, corresponding to that one of V_2O_5. After reaction at 400 °C, instead, the presence of vanadium oxides in different oxidation states (namely V_2O_5, VO_2, V_2O_3, with also possible traces of V_6O_{13} and V_4O_7) was observed. Finally, after reaction at 550 °C, the reflections typical of V_2O_5 were no longer present, and the only crystalline compounds were VO_2 and V_2O_3.
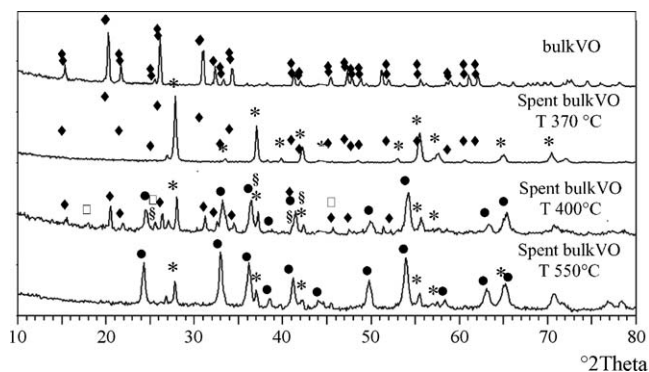

Fig. 5. X-ray diffraction patterns of fresh bulkVO and of spent bulkVO after reaction at 370, 400 and 550 °C. Symbols: (◆) V_2O_5, (●) V_2O_3, (*) VO_2, (§) V_4O_7 and (□) V_6O_{13}.

The formation of reduced vanadium oxides was a consequence of the development of a reductive environment that occurred at high temperature, after total oxygen conversion had been attained. This implies that the catalyst present in the lower part of the bed was different from that one closer to the reactor inlet, operating in the presence of gas-phase oxygen.

If this hypothesis is correct, the WGS reaction requires a substantially oxygen-free environment, otherwise vanadium oxide is in its oxidized form. This implies that oxygen has to be fed in a sub-stoichiometric amount with respect to that one required for the oxidation of the hydrocarbon to CO and H_2O. The propane/O_2 stoichiometric ratio for CO/H_2O production is equal to 1/3.5. With molar ratio 1/1 (like the one employed in tests of Figs. 1–4) O_2 was the limiting reactant; the consequence of this was that the maximum propane conversion obtained was low. On the other hand, the presence of unconverted hydrocarbon generated the reducing environment that was necessary for the in situ formation of the reduced vanadium oxide in the lower part of the catalytic bed.

Tests were carried out with different feed composition, in order to check whether it was possible to increase the amount of H_2 produced, with variation of either the propane-to-oxygen feed ratio, or by changing the reactants concentration. In fact, it is expected that a too low concentration of oxygen (with respect to the hydrocarbon fed) might give a low conversion of the hydrocarbon, with a consequently lower amount of hydrogen produced. Excessive amount of oxygen, instead, besides making the feed mixture approach the flammable area, might cause (i) an incomplete conversion of oxygen itself, so hindering the development of conditions favourable for WGS, and (ii) the possible preferred formation of CO_2 rather than CO in the aerobic reactor section, that would finally hinder the occurrence of WGS. So, the ratio between reactants not only affects the kinetics of the reaction, but also controls the nature of the active phase, and its in situ evolution.

Results of tests carried out at the following feed composition: (i) 20% propane and 20% oxygen (the same conditions used for tests in Figs. 1 and 2), (ii) 55% propane and 25% oxygen and (iii) 10% propane and 10% oxygen, are reported in Fig. 6. The propane and oxygen conversion (Fig. 6, top), and the yield to hydrogen (Fig. 6, bottom; H_2 yield: (0.25 H_2 concentration/inlet propane concentration)), are plotted as functions of the reaction temperature. In all cases H_2 began to form when total oxygen conversion was reached. This further confirms that the generation of H_2 necessitates a fraction of catalytic bed working under anaerobic conditions.

In the case of tests done with propane-to-oxygen feed ratio equal to 1, the conversion of oxygen and propane and the yield to H_2 were the same with the two different feed compositions; the concentration of H_2 in the exit stream was clearly the lower in the case of tests run with 10% propane concentration. Different was the case with the hydrocarbon-richer feed and propane-to-oxygen feed ratio equal to 2.2. The total conversion of oxygen was reached at much lower temperature than with the propane-leaner feed. Furthermore, as a consequence of the less oxygen available, (i) propane conversion levelled off at lower temperature (350 °C), (ii) maximum propane conversion was
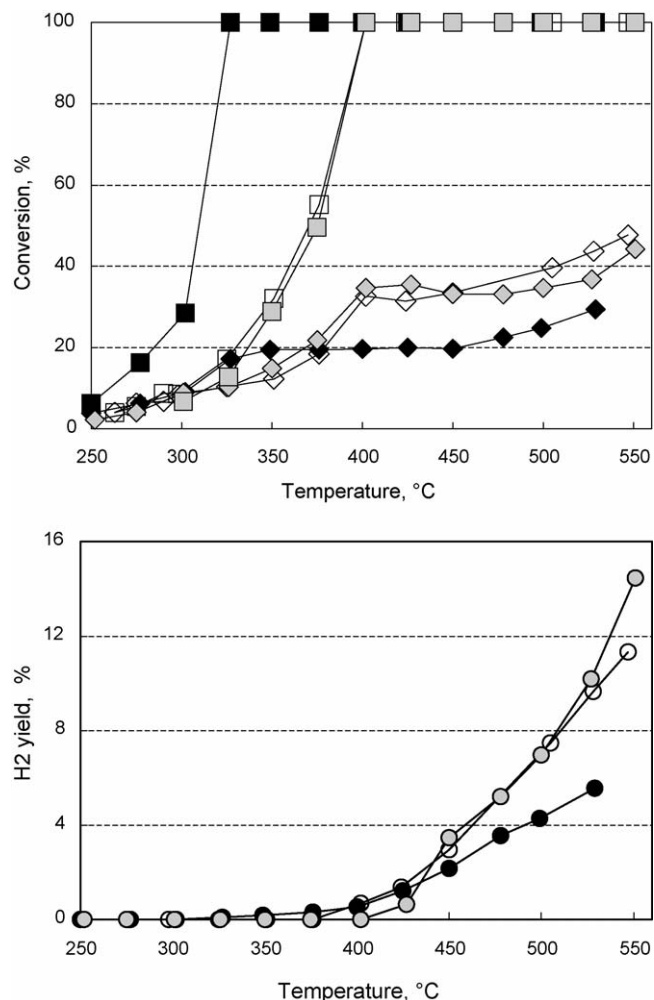

Fig. 6. Conversion of propane (rhombus) and conversion of oxygen (square) as functions of temperature (top); hydrogen concentration in the exit stream (circles) as function of temperature (bottom). Catalyst: bulkVO. Feed composition: 10% propane and 10% oxygen (grey symbols); 20% propane and 20% oxygen (white symbols); 55% propane and 25% oxygen (black symbols).

lower and (iii) hydrogen began to form at lower temperature. The yield to H_2 was lower than with the hydrocarbon-leaner conditions, but its concentration in the outlet stream was higher.

All samples, when downloaded after reaction under conditions of total oxygen conversion, contained V_2O_4, V_2O_3 and an amount of coke comprised between 0.5 and 0.7 wt.% C.

In order to investigate the catalytic properties of the different vanadium oxides that developed inside the catalytic bed as a consequence of the total consumption of oxygen, tests were carried out by feeding a gaseous mixture containing 9% CO, 9% H_2O and 82% N_2. The reaction was first carried out with fresh bulkVO. Then, the same catalyst was pre-reduced by running the reaction of propane oxidation under those conditions that led to total oxygen conversion (T, 550 °C; feed, 20% propane and 20% oxygen). Finally, the CO/H_2O/N_2 mixture was fed on the pre-reduced catalyst. The nature of the vanadium oxide in each test was then confirmed by XRD characterization of the corresponding spent catalysts. In the case of test done with fresh bulkVO the catalyst was still V_2O_5,

while in the case of test done with the pre-reduced catalyst the only compound detected in the spent sample was V_2O_3. In the former case, the conversion of CO at 450 °C was 2–3%, with total selectivity to CO_2 and no formation of H_2; this indicates that V_2O_5 had very low activity in the WGSR. On the contrary, with the pre-reduced bulkVO the conversion of CO was equal to 32–35%, with total selectivity to CO_2 and a molar concentration of H_2 equal to 2.7%, that corresponds to a H_2 yield of 30%. These data confirm that the catalytic behaviour of bulkVO in propane oxidation (Fig. 2) derived from the development of reduced vanadium oxides in the fraction of catalytic bed operating under anaerobic conditions.

3.3. The characterization of catalysts: laser Raman spectroscopy

In literature, monolayer surface coverage, defined as the maximum amount of amorphous or two-dimensional vanadia in contact with the oxide support, has been experimentally determined by several techniques, since the completion of the monolayer precedes the formation of crystalline V_2O_5 [33–38]. It corresponds to 7–8 VO_x/nm^2 for alumina and to 0.7 VO_x/nm^2 for silica [34,36–38], even though under certain conditions this value can be improved [39]. Also, it is generally believed that V is present as V^{5+} [37].

For low vanadium oxide loading, the V species supported on silica exists as an isolated and distorted VO_4 units, with a single V=O terminal bond (characterized by a Raman band at 1037 cm^{-1}) and three bridging bonds connected to the silica support [19,34,37,40–45]. In the dehydrated state, this species is the only present. Upon hydration, the surface V species changes coordination from VO_4 to VO_5 or VO_6. The vanadium oxide gives rise to Raman bands at 150, 263, 323, 418, 512, 670–700 and 990–1016 cm^{-1}, characteristic of a hydrated species; the 1016 cm^{-1} band is characteristic of a terminal V=O bond that is partially dehydrated by the laser beam. The molecular structure of the fully hydrated samples having high active phase content, resembles that of the $V_2O_5 \cdot nH_2O$ gels, rather than V_2O_5 crystallites; they consist of chain or two-dimensional polymers with highly distorted VO_5 connected via V–OH–V bridges [39].

In the case of alumina-supported catalysts, it is assumed that the Raman band at around 1030 cm^{-1} is related to the isolated V=O bond in VO_x units (it may fall at lower wavenumber depending on the degree of hydration), while the band at around 915 cm^{-1} is due to V–O–V stretching vibration, and is thus typical of polymeric vanadate dispersed over alumina [36,42,46–48].

Raman spectra of our calcined supported samples are shown in Fig. 7. The formation of bulk V_2O_5 was observed in all samples with overall loading above 7 wt.% V_2O_5 content. X-ray diffraction patterns (not shown) confirmed the presence of crystalline V_2O_5 in SiV15, AlV10 and AlV15. In spectra of SiV2 and AlV2 (not reported), no clear signal attributable to any V species was present. Main differences between the two series of samples were observed with SiV7 and AlV7; while in the case of the silica-supported catalyst bands are those
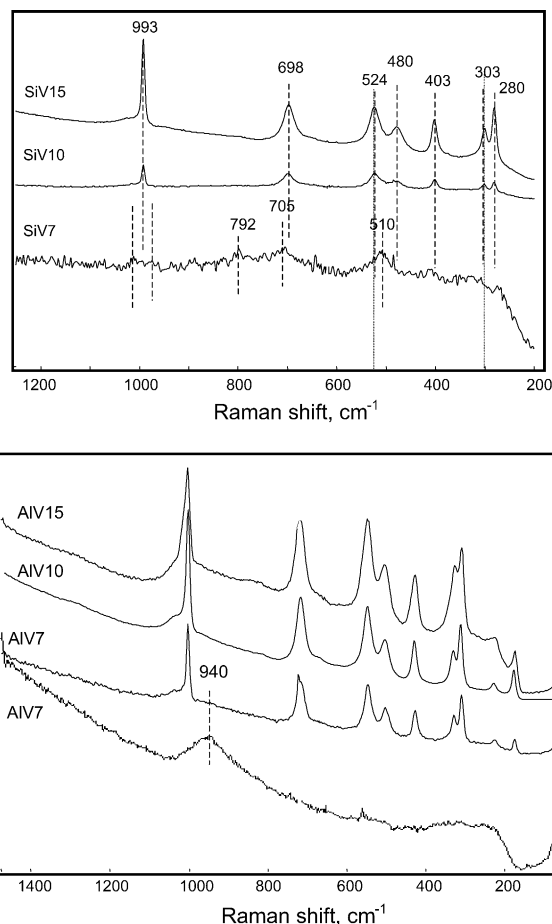

Fig. 7. Raman spectra of calcined SiVx (top) and AlVx (bottom).

typical of hydrated vanadium oxide, in AlV7 the band at 940 cm^{-1} is attributable to hydrated polymeric vanadate species. This sample, however, was non-homogeneous, and when the laser beam was focused on other particles, the spectrum corresponded to that one of bulk vanadium oxide. The spectra agree with literature indications about the property of alumina to yield polyvanadates species. On the contrary, this is not observed in the case of silica-supported systems, for which V clustering into bulk vanadium oxide is preferred. However, it has to be mentioned that recently Weckhuysen and coworkers [49,50] reported that the observed vibrational frequencies in the range 900–1100 cm^{-1} can be assigned to V=O (1030 cm^{-1}), O–O (915 cm^{-1}) and Si–O–V (980 cm^{-1}) without invoking the presence of polymeric species. The model proposed can be described as a chemisorbed Si–O–V=O(O$_2$) species. Therefore, the attribution of the 915 cm^{-1} band to V–O–V in polymeric vanadate, especially evident in alumina-supported systems, might not be valid. Other authors recently attributed this band to the Al–O–V stretching mode [51].

In summary, the following V species were present in the two series of supported samples:

(a) In samples containing 2 wt.% V_2O_5 (SiV2 and AlV2), literature data indicate the formation of an isolated

VO_x, chemically bound to the support. In fact the amount of vanadium oxide loaded corresponds to a surface density of ≈ 0.5 VO_x/nm^2 for SiV2 (close to the limit value of 0.7 for silica-supported vanadium oxide) and of ≈ 0.6 VO_x/nm^2 for AlV2.

(b) In samples containing 7 and 10 wt.% V_2O_5, the nature of the V species was different depending on the support type. In SiV7 and SiV10, bulk vanadium oxide formed. In the case of AlV7 polyvanadate species and bulk vanadium oxide formed, while AlV10 also had crystalline V_2O_5.

(c) In samples containing 15 wt.% V_2O_5 (SiV15 and AlV15) the prevailing species was crystalline V_2O_5.

The density of vanadium oxide in all AlVx samples was lower than the limit value of 7 VO_x/nm^2, and hence the prevailing formation of polyvanadates should be expected. This might indicate that the method employed for catalysts preparation is not very effective to achieve a good dispersion of vanadium oxide on γ-Al_2O_3.

The permanence of catalysts in the reaction environment led to an increase of the dispersion of the active phase, especially for alumina-supported samples. This is evident in Fig. 8, which reports the Raman spectra of spent AlV15 and SiV15; the catalysts were downloaded after reaction at high temperature, i.e., under conditions of total oxygen conversion. It is shown that the bands attributable to bulk vanadium oxide in the spectrum of AlV15 disappeared, while the band at 930 cm^{-1} formed. This indicates that the permanence in the reaction environment led to the spreading of bulk vanadium oxide to form polymeric vanadate species dispersed over alumina, probably because of (i) the particle temperature higher than that of the gas-phase, due to the heat developed by the strongly exothermic reactions, and (ii) the dynamic reaction environment. Two strong bands also were present, at 1600 and 1380 cm^{-1}, that can be attributed to the graphitic-like coke accumulated on the catalyst surface [52]. The same bands were absent in the case of spent SiV15; this confirms indications given by catalytic measurements, of a greater accumulation of
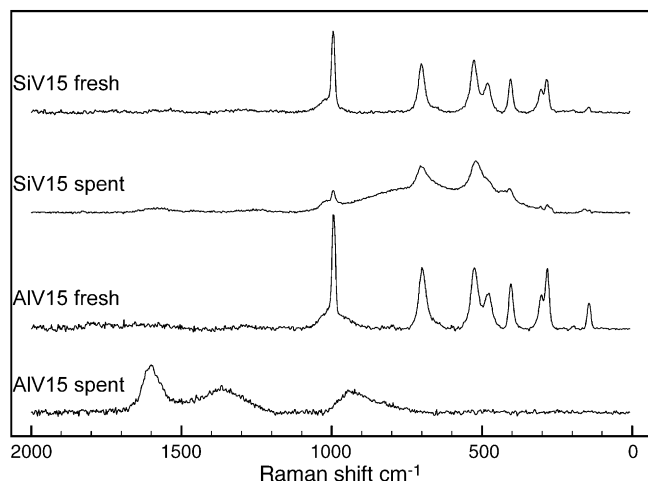
coke with AlV15 than with SiV15. Furthermore, the intensity of bands relative to V_2O_5 was considerably lower in spent SiV15 than in the fresh sample. Since there was no new band in the 900–1000 cm^{-1} range, this suggests a modification of crystalline vanadium oxide, such as a partial amorphization. The XRD pattern of spent SiV15 (not shown) evidenced the absence of reflections relative to crystalline V_2O_5, that were instead evident in the pattern of the corresponding calcined catalyst.

3.4. The characterization of catalysts: thermal-programmed-reduction and re-oxidation

Figs. 9–11 report the TPR and TPR-O (TPO after the TPR) profiles of samples. In literature, a reduction peak occurring at 430 °C for silica-supported vanadium oxide has been attributed to surface vanadia phase, and a second peak at 430–510 °C to crystalline V_2O_5 [53]. Other authors attributed a reduction peak at 460 °C to a surface species and peaks at 540 and 580 °C to reduction of bulk-like vanadia [54]. In one sample with very low vanadium oxide content, a peak with maximum at 515 °C was attributed to the reduction of isolated VO_x units [55–57]. In the case of alumina-supported systems, for very low vanadium oxide loading a TPR peak with maximum at 550 °C was found [55–57]; the H/V atomic ratio was close to 2, indicating a reduction of V^{5+} to V^{3+}. With 5 and 10% V_2O_5/Al_2O_3, the T_{max} was at 493 °C (H/V 1.75 and 1.66, respectively), while with 5 and 10% V_2O_5/SiO_2 it was at 526 and 540 °C (H/C 1.88 and 2.00), respectively. The authors concluded that in the case of

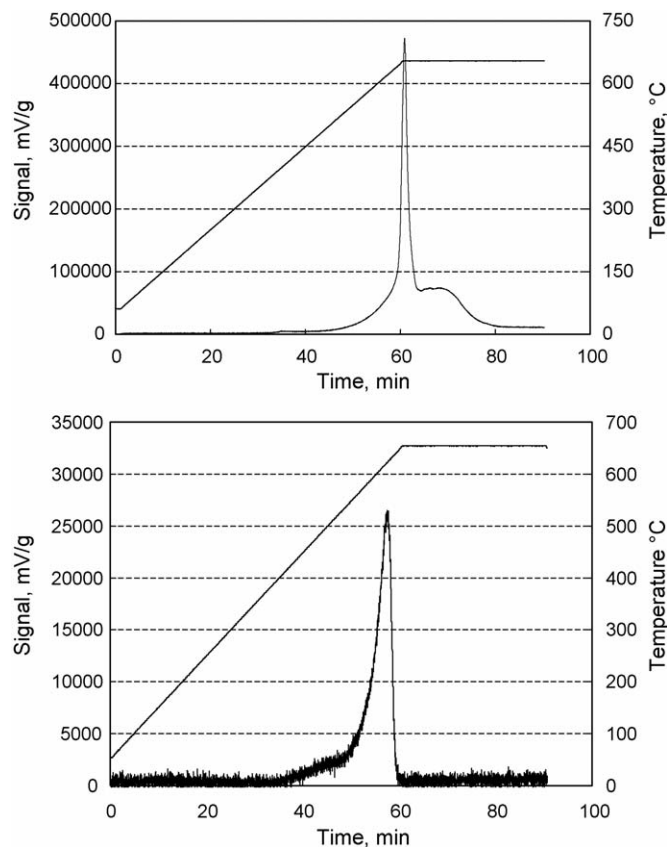Fig. 8. Raman spectra of AlV15 and SiV15 before and after reaction.

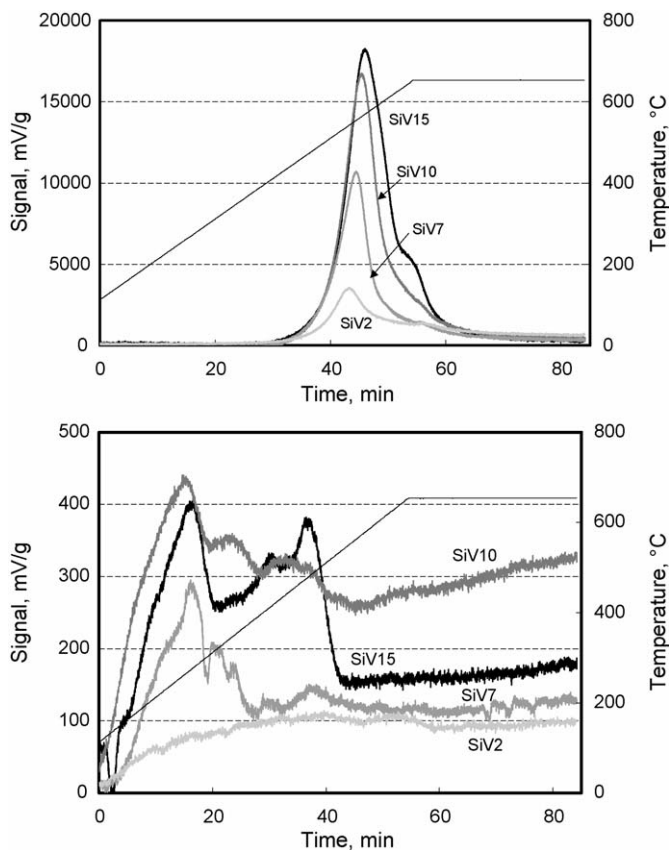Fig. 9. TPR profile (top) and TPR-O profile (bottom) of bulkVO.

Fig. 10. TPR profile (top) and TPR-O profile (bottom) of SiVx.

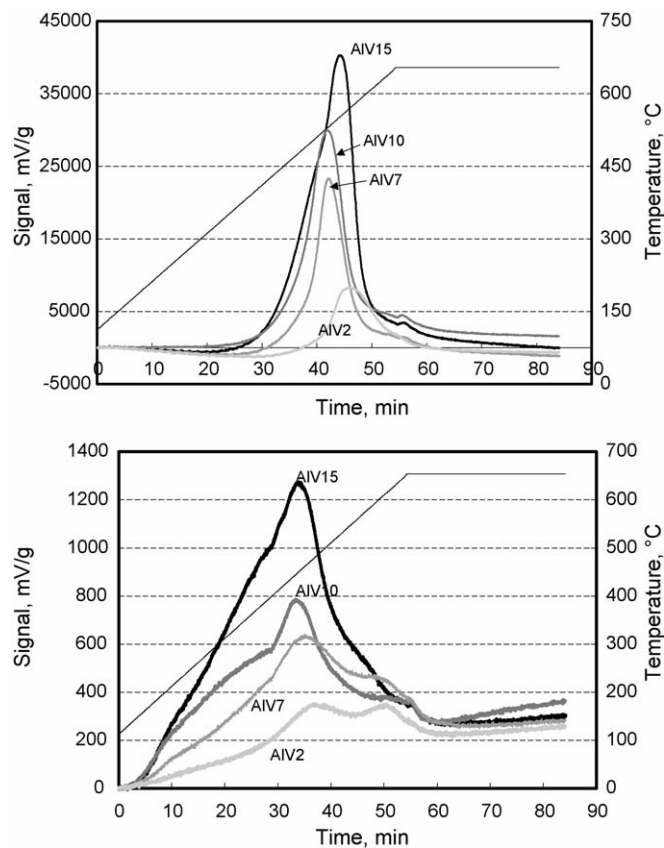Fig. 11. TPR profile (top) and TPR-O profile (bottom) of AlVx.

silica all V^{5+} was reduced to V^{3+}, while in the case of alumina some V^{5+} was reduced to V^{4+}, that was stabilized in this oxidation state [55–57].

With our samples, in the case of bulk VO (Fig. 9) the peak of reduction fell at higher temperature than the corresponding peak for supported samples (Figs. 10 and 11). The reduction began slowly at 450 °C, and accelerated at 600 °C; in correspondence of the isothermal step, the reduction rate abruptly decreased, and the reduction was then completed within less than 1 h. When the same sample was treated in a flow of diluted oxygen after the TPR step (Fig. 9, bottom), the re-oxidation was completed at 650 °C, before the start of the final isothermal step.

In the case of silica-supported samples (Fig. 10, top), the profile showed one major reduction peak, the position of which was not much affected by the amount of active phase. One second minor component was present at high temperature, beginning before the isothermal step, and more evident in SiV15; on the basis of literature indications, the latter is attributable to crystalline V_2O_5.

The TPO profiles (not reported) evidenced the absence of any O_2 uptake, suggesting that either all V was present as V^{5+}, or any reduced V species, if present, was not oxidizable in the temperature range used for TPO. Fig. 10 (bottom) reports the TPO profiles of pre-reduced samples (TPR-O); these profiles allowed an easier identification of the peaks attributable to the various V species. SiV2 did not evidence any clear O_2 uptake; it

is not possible to say if this was due to the fact that the re-oxidation occurred over a wide range of temperature, making the oxidation peak not distinguishable from the baseline, or to the fact that the isolated V species, once reduced, could not be re-oxidized. TPR-O profiles of SiV7, SiV10 and SiV15 evidenced at least two major components, (i) between 100 and 300 °C, and (ii) above 300 °C. The latter was particularly evident in SiV15, while it was substantially absent in SiV7. It is possible to tentatively attribute the first TPO peak to the re-oxidation of amorphous bulk vanadium oxide, and the second one to the re-oxidation of crystalline vanadium oxide.

The TPR profiles of alumina-supported samples (Fig. 11, top) evidenced some differences with respect to profiles of SiVx. The isolated VO_x species (present in AlV2) gave a peak of reduction that fell at higher temperature than the corresponding peak in SiV2. This indicates that the reducibility of this species is easier when it is bound to silica. The polyvanadate species (the prevailing one in AlV7) was instead characterized by a reduction peak with maximum around 535 °C, that is approximately 20–25° less than the temperature of reduction of the main species in SiV7. The reduction profile of AlV10 was not much different from that one of AlV7, while the peak of AlV15 had an additional high-temperature contribution (T_{max} =574 °C), that can be attributed to the reduction of bulk vanadium oxide. In both AlV10 and AlV15 the maximum of the reduction peak fell at lower temperature than in SiVx having the same V_2O_5 content: 536 °C for AlV10

versus 568 °C for SiV10, and 557 °C for AlV15 versus 574 °C for SiV15. This confirms the easier reduction of vanadium oxide when deposited on alumina (except for the isolated VO_x species). However, it is worth noting that apparently the main contribution to the reduction peak in AlV15 was due to bulk vanadium oxide, rather than to polyvanadates. Also with these samples the TPO tests did not evidence any O_2 uptake.

The TPR-O (TPO after TPR tests) profiles of AlVx are shown in Fig. 11 (bottom); also in this case, these profiles allowed a better distinction between the different V species, the reducibility of which, instead, could not be clearly distinguished in TPR profiles. Three contributions were present, falling in different temperature ranges: (i) the high-T peak, well evident in AlV2, is attributable to the re-oxidation of the isolated V species, (ii) the medium-T peak to polyvanadates and (iii) the low-T peak to bulk vanadium oxide. The presence of two peaks in the profile of sample AlV2 may suggest the formation of polyvanadates, too. The comparison with TPR-O profiles of SiVx indicates that the reduced V species in silica-supported catalysts are more easily re-oxidizable than those in AlVx.

Fig. 12 reports the amount of H_2 consumed per gram of catalyst in TPR tests for the SiVx and AlVx; the values obtained by reduction of the same catalysts downloaded after reaction at 550 °C (that is, under conditions at which total oxygen conversion was reached) are also reported in the figures. The stoichiometries for the corresponding theoretical values, the 2-electron reduction of V^{5+} to V^{3+} and the 1-electron reduction of V^{5+} to V^{4+} are given for reference. It is shown that in the case of AlVx the stoichiometry coincided with the theoretical one for the reduction of V^{5+} to V^{3+}. On the contrary, with SiVx the experimental amount was very close to the theoretical one for the 1-electron reduction; therefore, in this case the V^{5+} ions were reducible to V^{4+}, but not to V^{3+}. This difference likely derives from the nature of the interaction that develops between the active phase and the support. These results disagree in part with literature indications, that report a complete reduction of V^{5+} to V^{3+} for silica-supported vanadium oxide catalysts [55–57]. In the latter case, however, catalysts were calcined at lower temperature than our samples; this might be one reason for a different stabilization of the V species towards reduction by H_2.

The amount of O_2 uptake as measured in TPR-O tests confirmed the indications given by TPR measurements. In average, the amount of O_2 consumed corresponded to the less than 1-electron re-oxidation for SiVx, and to the 2-electron re-oxidation for AlVx.

When the TPR tests were carried out on samples downloaded after reaction (reduction profiles not reported), the amount of H_2 consumed was similar to that one of fresh catalysts for SiVx, while it was less than half of the amount obtained with the corresponding fresh samples for AlVx. This means that in the former case vanadium was still in a high oxidation state (close to V^{5+}). It is worth noting that the TPR tests were carried out on samples downloaded after reaction under conditions that led to total oxygen consumption, that is a reductive environment, at least for the part of catalytic bed operating in the absence of O_2.
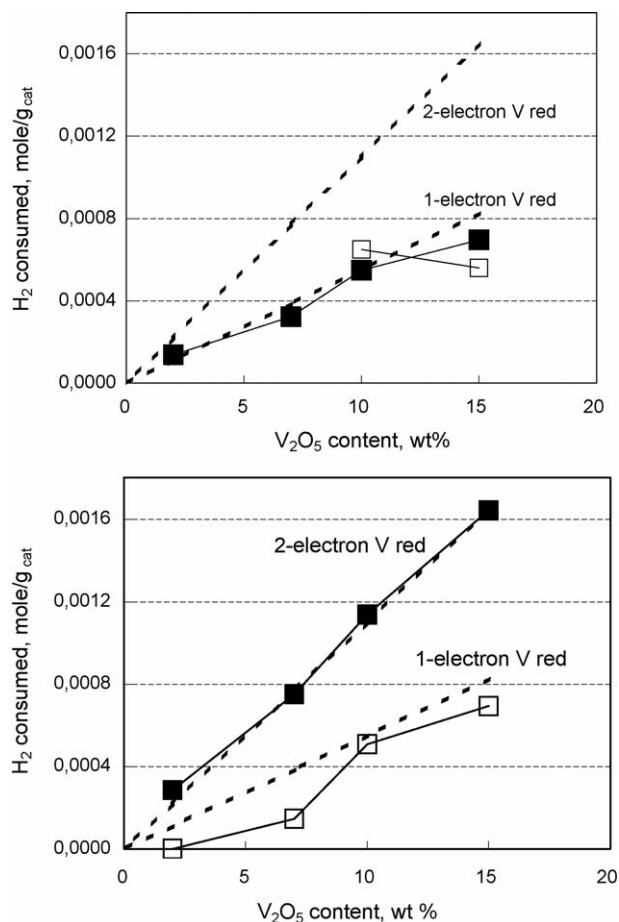

Fig. 12. Amount of H_2 consumed per unit weight of catalyst in TPR tests of calcined samples (full squares) and of samples downloaded after reaction under conditions of total oxygen conversion (open squares): SiVx (top) and AlVx (bottom). Dotted lines: stoichiometry of reference reductions.

For example, in the case of SiV15 the reduction profile of the spent catalyst was the same as that one of the fresh sample, except for the high-temperature shoulder, that was absent in spent SiV15. This confirms indications given by Raman spectrum (Fig. 8) and XRD pattern of a modification of features for crystalline V_2O_5 in spent SiV15.

On the contrary, in the case of spent AlVx the average oxidation state for V was close to 4+. A lower V oxidation state under reaction conditions for AlVx than for SiVx may be the reason for the greater accumulation of coke with the former catalysts. Coke might also contribute to H_2 consumption in TPR tests however, the shape of TPR profiles of spent AlVx was quite similar to that of corresponding fresh catalysts, and no evidence was obtained for an additional peak attributable to coke hydrogenation.

Literature gives contrasting indications about the V valence state under reaction conditions; for instance, Gao et al. [58] report that in both silica- and alumina-supported vanadium oxide, when used as catalysts for alkane ODH, there is a very limited reduction of V^{5+}. Argyle et al. [59] found that in alumina-supported catalysts the extent of V reduction during propane ODH was much lower than that corresponding to the formation of V^{4+} or V^{3+}. Moreover, only a fraction of the

reduced V sites was active in catalytic turnovers. On the contrary, Ruitenbeek et al. [60] reported that in alumina-supported vanadium oxide the removal of O_2 from the CO/O_2 feed caused the reduction of V to V^{3+}, which subsequently migrated into the γ-Al_2O_3 lattice; the migration was reversible, and the V^{5+} sites was restored by re-oxidation. In general, in the redox mechanism involved in alkane ODH, the reduction is considered the rate-limiting step, since the kinetic constants for reduced sites re-oxidation are greater than the reduction ones by C–H bond activation. Therefore, usually relationships between ODH reaction rates and reducibility of metal oxides, typically measured by H_2-TPR, have been searched for and reported [61–64]. However, this approach has been confuted by Iglesia and coworkers [65], who reported that indeed the mechanisms for the electron transfer during C–H bond activation and during the ligand-to-metal charge-transfer process suggest that the stability of activated complexes in C–H bond dissociation step depends sensitively on the ability of the active oxide to transfer electrons from lattice oxygen atoms to metal centers.

Our results indicate that the average oxidation state for V, under those reaction conditions that favour the formation of H_2 (total oxygen conversion and high temperature), was higher in SiV_x than in AlV_x. This likely derived from the lower reducibility of V species in the former samples. With both systems, the V species that developed catalyzed the dehydrogenation of propane, but were not active in the WGS reaction.

The different reducibility and re-oxidizability of V in silica-supported and alumina-supported systems may also have implications on catalytic performance under low-temperature conditions. For instance, from the kinetic point of view this may be the reason for a different balance between the rates for the two steps of V reduction and V re-oxidation in the catalytic redox cycle. If the kinetic constant for V reduction by propane is smaller that that one for V re-oxidation, the two rates are in balance only for a very low concentration of reduced V sites, and the catalyst operates with a high V oxidation state. If instead the re-oxidation of V is the slower step, the catalyst is more reduced. A different nature of the rate-determining step can justify the differences in activity between the two series of supported samples.

4. Conclusions: relationships between chemical–physical characteristics and catalytic performance

Bulk vanadium oxide, silica-supported and alumina-supported vanadium oxide were tested as catalysts for propane oxidation, in order to find conditions under which H_2 is produced, and to determine which are the catalyst properties that favour its formation. The following considerations are worth of mention:

(1) The differences in activity for propane oxidation (15 wt.% V_2O_5/γ-Al_2O_3 > 15 wt.% V_2O_5/SiO_2) derived from the different reducibility an re-oxidizability of vanadium oxide, when spread either over silica or over alumina. This also implied that the average oxidation state of V under reaction conditions was a function of the support type. With silica-supported catalysts, V was present mainly as V^{5+} even under conditions of total oxygen conversion, whereas in alumina-supported samples V was considerably more reduced.

(2) Bulk V_2O_5 was less reducible and less re-oxidizable than dispersed vanadium oxide; its high activity in propane oxidation likely derived from the quick bulk-to-surface diffusion of O^{2-}, that allowed the replenishment of the surface concentration of V^{5+} sites. This however was no longer true under conditions at which total oxygen consumption was reached; in this case, reduced vanadium oxides developed under reaction conditions.

(3) The amount of hydrogen produced under conditions of total oxygen consumption followed the rank: V_2O_5 > 15 wt.% V_2O_5/γ-Al_2O_3 > 15 wt.% V_2O_5/SiO_2. This was due to the fact that with bulk vanadium oxide, operation under conditions of total oxygen conversion led to the development of V_2O_3; the latter was active in the WGSR, where the reactants for this reaction formed in the fraction of bed where V_2O_5 catalyzed the oxidation of propane. In supported samples, instead, the WGS reaction did not occur, due to the fact that the active phase was made either of V^{5+} sites in the case of silica-supported samples, or of V^{4+} with alumina-supported samples. The difference between alumina and silica-supported catalysts, instead, was due to the different amount of coke that accumulated on catalysts; the latter was the higher in alumina-supported catalysts, either because of a direct contribution of the support, or due to the lower oxidation state of V under reaction conditions.

References

[1] S. Albertazzi, P. Arpentinier, F. Basile, D. Gallo, G. Fornasari, D. Gary, A. Vaccari, Appl. Catal. A 247 (2003) 1.
[2] E.L. Sørensen, J. Perregaard, Stud. Surf. Sci. Catal. 147 (2004) 7.
[3] D.A. Hickman, L.D. Schmidt, J. Catal. 138 (1992) 267.
[4] D.A. Hickman, L.D. Schmidt, Science 259 (1993) 343.
[5] K.L. Hohn, L.D. Schmidt, Appl. Catal. A 211 (2001) 53.
[6] P.K. Bakkerud, J.N. Gol, K. Aasberg-Petersen, I. Dybkjaer, Stud. Surf. Sci. Catal. 147 (2004) 13.
[7] C.M. Chen, D.L. Bennett, M.F. Carolan, E.P. Foster, W.L. Schinski, D.M. Taylor, Stud. Surf. Sci. Catal. 147 (2004) 55.
[8] S. Ayabe, H. Omoto, T. Utaka, R. Kikuchi, K. Sasaki, Y. Teraoka, K. Educhi, Appl. Catal. A 241 (2003) 261.
[9] P. Aghalayam, Y.K. Park, D.G. Vlachos, Catalysis 15 (2000) 98.
[10] G. Groppi, W. Ibashi, E. Tronconi, P. Forzatti, Chem. Eng. J. 82 (2001) 57.
[11] A.T. Ashcroft, P.D.F. Vernon, M.L.H. Green, Nature 344 (1990) 319.
[12] A.P.E. York, T. Xiao, M.L.H. Green, Top. Catal. 22 (2003) 345.
[13] D. Sanfilippo, I. Miracca, U. Cornaro, F. Mizia, A. Malandrino, V. Piccoli, S. Rossini, Stud. Surf. Sci. Catal. 147 (2004) 91.
[14] K. Otsuka, A. Mito, S. Takenaka, I. Yamanaka, Int. J. Hydrogen Energy 26 (2001) 191.
[15] T. Zhang, M.D. Amiridis, Appl. Catal. A 167 (1998) 161.
[16] B. Grzybowska-Swierkosz, F. Trifirò, J.C. Vedrine, Appl. Catal. A 157 (1997), Special issue on "Vanadia catalysts for selective oxidation of hydrocarbons", and papers therein.

[17] S. Albonetti, F. Cavani, F. Trifirò, Catal. Rev. -Sci. Eng. 38 (1996) 413.

[18] F. Cavani, F. Trifirò, in: M. Baerns (Ed.), Basic Principles in Applied Catalysis, Springer, Berlin, 2004, p. 22.

[19] B.E. Weckhuysen, D.E. Keller, Catal. Today 78 (2003) 25.

[20] J. Haber, M. Witko, R. Tokarz, Appl. Catal. A 157 (1997) 3.

[21] T. Blasco, J.M. Lopez Nieto, Appl. Catal. A 157 (1997) 117.

[22] F. Cavani, F. Trifirò, Catal. Today 24 (1995) 307.

[23] H.H. Kung, Adv. Catal. 40 (1994) 1.

[24] E.A. Mamedov, V. Cortes Corberan, Appl. Catal. A 127 (1995) 1.

[25] J.C. Vedrine, G. Coudurier, J.M.M. Millet, Catal. Today 33 (1997) 3.

[26] B. Grzybowska-Swierkosz, Top. Catal. 21 (2002) 35.

[27] M.Y. Sinev, Z.T. Fattakhova, Y.P. Tulenin, P.S. Stennikov, V.P. Vislovskii, Catal. Today 81 (2003) 107.

[28] N. Ballarini, F. Cavani, C. Cortelli, C. Giunchi, P. Nobili, F. Trifirò, R. Catani, U. Cornaro, Catal. Today 78 (2003) 353.

[29] N. Ballarini, F. Cavani, M. Ferrari, R. Catani, U. Cornaro, J. Catal. 213 (2003) 95.

[30] N. Ballarini, F. Cavani, A. Cericola, C. Cortelli, M. Ferrari, F. Trifirò, R. Catani, U. Cornaro, Stud. Surf. Sci. Catal. 147 (2004) 649.

[31] N. Ballarini, F. Cavani, A. Cericola, C. Cortelli, M. Ferrari, F. Trifirò, G. Capannelli, A. Comite, R. Catani, U. Cornaro, Catal. Today 91–92 (2004) 99.

[32] I. Lima Junior, J.-M.M. Millet, M. Aouine, M. do Carmo Rangel, Appl. Catal. A 283 (2005) 91.

[33] G.C. Bond, S.F. Tahir, Appl. Catal. 71 (1991) 1.

[34] G. Deo, I.E. Wachs, J. Haber, Crit. Rev. Surf. Chem. 4 (1994) 141.

[35] B.M. Weckhuisen, I.E. Wachs, J. Phys. Chem. 100 (1996) 14437.

[36] I.E. Wachs, Catal. Today 27 (1996) 437.

[37] I.E. Wachs, B.M. Weckhuysen, Appl. Catal. A 157 (1997) 67.

[38] G. Deo, I.E. Wachs, J. Catal. 146 (1994) 323.

[39] X. Gao, S.R. Bare, B.M. Wechkuysen, I.E. Wachs, J. Phys. Chem. B 102 (1998) 10842.

[40] N. Das, H. Eckert, H. Hu, I.E. Wachs, J.F. Walzer, F.J. Feher, J. Phys. Chem. 97 (1993) 8240.

[41] G.T. Went, S.T. Oyama, A.T. Bell, J. Phys. Chem. 94 (1990) 4240.

[42] L.J. Burcham, G. Deo, X. Gao, I.E. Wachs, Top. Catal. 11/12 (2000) 85.

[43] I.E. Wachs, Catal. Today 100 (2005) 79.

[44] J.M. Jehng, G. Deo, B.M. Weckhuysen, I.E. Wachs, J. Mol. Catal. A 110 (1996) 41.

[45] C.B. Wang, G. Deo, I.E. Wachs, J. Catal. 178 (1998) 640.

[46] M.A. Vuurman, I.E. Wachs, J. Phys. Chem. 96 (1992) 5008.

[47] S.T. Oyama, G.T. Went, K.B. Lewis, A.T. Bell, G.A. Somorjai, J. Phys. Chem. 93 (1989) 6786.

[48] B.M. Weckhuysen, J.M. Jehng, I.E. Wachs, J. Phys. Chem. B 104 (2000) 7382.

[49] J.N.J. van Lingen, O.L.J. Gijzeman, B.M. Weckhuysen, J.H. van Lenthe, J. Catal. 239 (2006) 34;
O.L.J. Gijzeman, J.N.J. van Lingen, J.H. van Lenthe, S.J. Tinnemans, D.E. Keller, B.M. Weckhuysen, Chem. Phys. Lett. 397 (2004) 277.

[50] D.E. Keller, F.M.F. de Groot, D.C. Koningsberger, B.M. Weckhuysen, J. Phys. Chem. B 109 (2005) 10223.

[51] N. Magg, B. Immaraporn, J.B. Giorni, T. Schroeder, M. Bäumer, J. Döbler, Z. Wu, E. Kondratenko, M. Cherian, M. Baerns, P.C. Stair, J. Sauer, H.-J. Freund, J. Catal. 226 (2004) 88.

[52] M.A. Banares, Raman spectroscopy, in: B.M. Weckhuysen (Ed.), In Situ Characterization of Catalytic Materials, American Scientific Publishers, 2004.

[53] F. Roozeboom, M.C. Mittelmeijer-Hazeleger, J.A. Moulijn, J. Medema, V.H.J. de Beer, P.J. Gellings, J. Phys. Chem. 84 (1980) 2783.

[54] M.M. Koranne, J.G. Goodwin, G. Marcelin, J. Catal. 148 (1994) 369.

[55] X. Gao, I.E. Wachs, J. Catal. 192 (2000) 18.

[56] X. Gao, S.R. Bare, J.L.G. Fierro, I.E. Wachs, J. Phys. Chem. B 103 (1999) 618.

[57] X. Gao, S.R. Bare, J.L.G. Fierro, M.A. Banares, I.E. Wachs, J. Phys. Chem. B 102 (1998) 5653.

[58] X. Gao, M.A. Banares, I.E. Wachs, J. Catal. 188 (1999) 325.

[59] M.D. Argyle, K. Chen, C. Resini, C. Krebs, A.T. Bell, E. Iglesia, J. Phys. Chem. B 108 (2004) 2345.

[60] M. Ruitenbeek, A.J. van Dillen, F.M.F. de Groot, I.E. Wachs, J.W. Geus, D.C. Koningsberger, Top. Catal. 10 (2000) 241.

[61] K. Chen, S. Xie, A.T. Bell, E. Iglesia, J. Catal. 198 (2001) 232.

[62] K. Chen, S. Xie, A.T. Bell, E. Iglesia, J. Catal. 195 (2000) 244.

[63] J.M. Lopez Nieto, J. Soler, P. Concepcion, J. Herguido, M. Menéndez, J. Santamaria, J. Catal. 185 (1999) 324.

[64] R. Grabowski, B. Grzybowska, K. Samson, J. Sloczynski, J. Stoch, K. Wcislo, Appl. Catal. A 125 (1995) 129.

[65] K. Chen, A.T. Bell, E. Iglesia, J. Catal. 209 (2002) 35.